DOI: 10.1002/chem.200800787

Metallobiological Necklaces: Mass Spectrometric and Molecular Modeling Study of Metallation in Concatenated Domains of Metallothionein

Jayna Chan,[a] Zuyun Huang,[a] Ian Watt,[b, c] Peter Kille,[b] and Martin Stillman*[a]

Abstract: The ubiquitous protein metallothionein (MT) has proven to be a major player not only in the homeostasis of Cu^{I} and Zn^{II}, but also binds all the Group 11 and 12 metals. Metallothioneins are characterised by the presence of numerous cys-x-cys and cys–cys motifs in the sequence and are found naturally with either one domain or two, linked, metal-binding domains. The use of chains of these metal–thiolate domains offers the possibility of creating chemically tuneable and, therefore, chemically dependent electrochemical or photochemical surface modifiers or as nanomachinery with nanomechanical properties. In this work, the metal-binding properties of the Cd_4-containing domain of α-rhMT1a assembled into chains of two and three concatenated domains, that is, "necklaces", have been studied by spectrometric techniques, and the interactions within the structures modelled and interpreted by using molecular dynamics. These chains are metallated with 4, 8 or 12 Cd^{II} ions to the 11, 22, and 33 cysteinyl sulfur atoms in the α-rhMT1a, αα-rhMT1a, and ααα-rhMT1a proteins, respectively. The effect of pH on the folding of each protein was studied by ESI-MS and optical spectroscopy. MM3/MD simulations were carried out over a period of up to 500 ps by using force-field parameters based on the reported structural data. These calculations provide novel information about the motion of the clustered metallated, partially demetallated, and metal-free peptide chains, with special interest in the region of the metal-binding site. The MD energy/time trajectory conformations show for the first time the flexibility of the metal–sulfur clusters and the bound amino acid chains. We report unexpected and very different sizes for the metallated and demetallated proteins from the combination of experimental data, with molecular dynamics simulations.

Keywords: cadmium · mass spectrometry · metallothionein · molecular dynamics · molecular modeling

Introduction

Metallothioneins (MTs) are an important class of metalloproteins that occur widely across all species and exhibit a remarkable ability to bind multiple metal ions. However, unlike other metal-binding metalloproteins, the metal-binding sites in metallothioneins are formed solely by metal–thiolate (M-Scys) connections through bridging and terminal cysteinyl sulfur ligands[1–9] and form as multimetal clusters. These clusters impart discrete, highly organised, three-dimensional domain structures into the metalloprotein as the peptide chain winds around the cluster sites, as seen in Figures 1–3. The coordination of the metal ions essentially imposes complete control of the secondary and tertiary structure that comprise the MT protein, given that removal of the metal ions strongly correlates with an almost complete loss of the secondary and tertiary structure of the protein as a whole, as monitored experimentally by CD spectroscopy.[3,9–11] Metallothioneins are an excellent example of metal-induced folding in which metallation dominates protein folding. However, recent studies[10] do indicate that the metal-free protein may adopt a loose, but specific, structure that predisposes the metal-free protein to rapid metallation.

MTs have been associated with metal homeostasis of Zn^{II} and Cu^{I} and detoxification of Cd^{II}, although their definite physiological function is still a matter of debate.[1–3,12–15] The mammalian MT proteins form with two metal-binding domains through coordination of all 20 of the cysteinyl sulfur atoms to a very wide range of divalent metal ions, primarily,

[a] Dr. J. Chan, Dr. Z. Huang, Prof. M. Stillman
Department of Chemistry, The University of Ontario
London, Ontario,, N6 A 5B7 (Canada)
Fax: (+1) 519-661-3022
E-mail: martin.stillman@uwo.ca

[b] Dr. I. Watt, Dr. P. Kille
Department of Biochemistry, University of Cardiff
Wales (UK)

[c] Dr. I. Watt
The Medical Research Council Dunn Human Nutrition Unit
Hills Road, Cambridge (UK)

but not exclusively, Group 11 and 12 metals, such as Cd^{II} and Zn^{II}, with stoichiometries for the divalent metals of M_3Scys_9 in the β domain and M_4Scys_{11} in the α domain.[4–8] The presence of cys–cys, cys-x-cys, and cys-x-y-cys, in which x and y are other amino acids, Figure 1, leads to the formation of these metal–thiolate clusters inside a tightly wrapped peptide chain.[3,5,6] The two isolated domains shown in Figure 2 are connected through a short linker region in the native βα mammalian protein with the two domains relatively isolated.[5] In addition to the detailed structural information known about Zn^{II} and Cd^{II} binding, mammalian proteins also bind all the other Group 11 and 12 metals, particularly, Hg^{II} and Cu^{I}, most likely also in two independent, metal–thiolate, clustered domains; more diverse metal binding also includes As^{III}.[16] Metallothioneins are thought to function biologically as intracellular distributors and mediators of the essential metals they bind.[1–2,12–15,17–18]

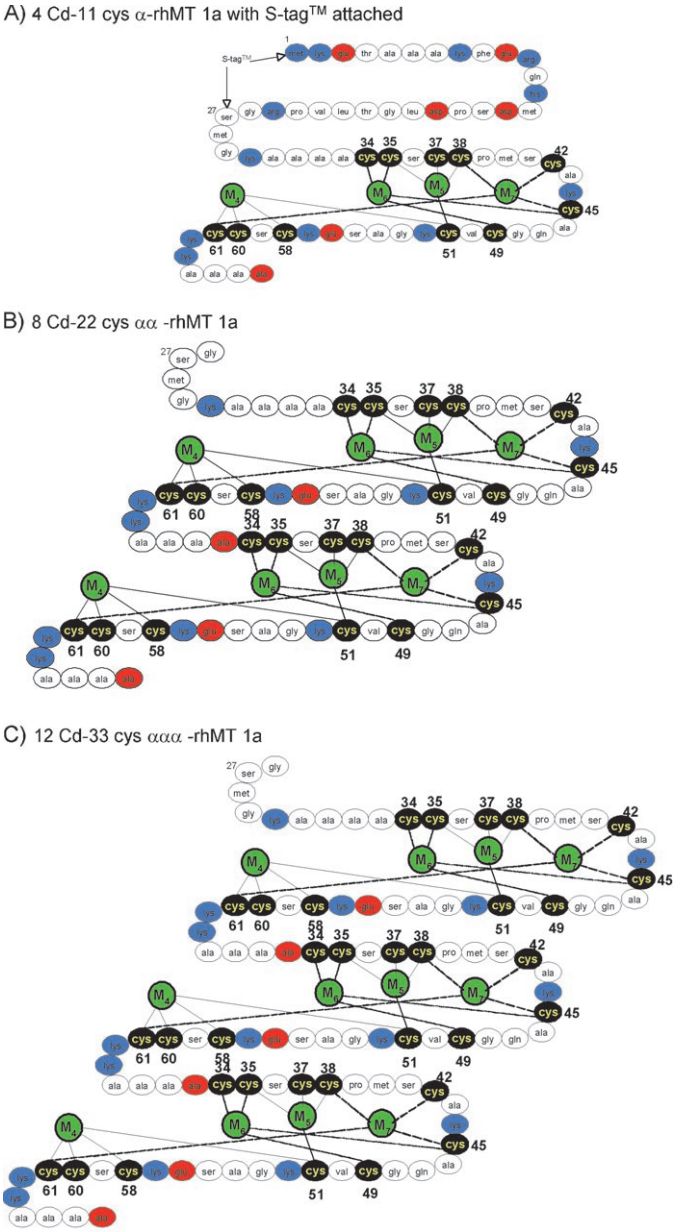

Figure 1. Sequences of A) the α domain, showing the sequence of the S-tag™ peptide, B) the αα domains and C) the ααα domains of recombinant human metallathionein-1a showing the proposed connectivities of four, eight and twelve divalent metal cations to the 11, 22 and 33 cysteinyl sulfur atoms, respectively. The numbers of the cysteines match those of rabbit liver MT2A and are consistent with the numbering scheme shown on the metal–thiolate clusters in Figure 2. The colouration of blue for basic amino acid residues and red for acidic amino acid residues is related to the location of protonation in the ESI-mass spectra, in which the protein is measured with charge states from +4 to +13, representing up to 13 protons. Note that only the α-rhMT1a protein has the S-tag™ attached in the ESI-MS data shown in this paper, the αα and ααα proteins have had the S-tag™ cleaved using thrombin, as described in the Experimental Section.

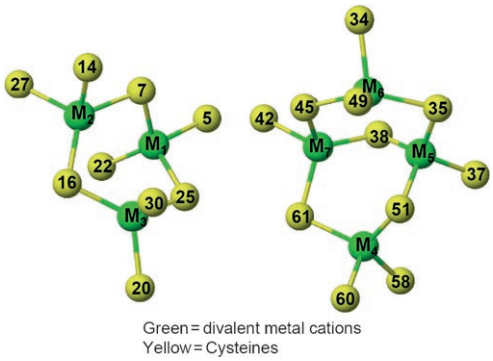

Figure 2. Metal–thiolate cores for Cd^{II} in the β (left) and α (right) domains of mammalian MT based on the connectivities from NMR spectroscopy and X-ray analysis with force-fields modified for both terminal and bridging thiolates.[4–8,22] In this study, only α domains have been used. Each metal is tetrahedrally coordinated by a mixture of bridging and terminal thiolates from the cysteine residues. The β domain core is shown for completeness as the structure is different.

Nature has provided this small MT molecule, which exhibits multi-faceted metal binding,[1–3,9–11] with a distinct arrangement of cysteine residues that predisposes metal specificity upon each domain, resulting in the formation of two separate domains in the mammalian protein. Whereas the mammalian and crustacean proteins bind Zn^{II} and Cd^{II} in two domains, yeast and many simpler systems bind metals in a single domain.[19] It is not clear what the biochemical reasons are for the evolution of a two-domain system. Reports of differential binding to the two domains suggest biological activity that is selective for either domain, but this is only one function. The connection between structure and function in MT also allows for the design of novel metal-binding molecules with high degrees of metal specificity as well as unusual structural properties, because the three-dimensional structure (both secondary and tertiary) is dominated by the metallation status.[4–8,10]

In this study, we have chosen concatenation as a way of studying the effects of domain number on metallation properties. We also wish to investigate the use of chains of domains as metallobiological "necklaces" with distinct and controllable chemical and physical properties, properties dictated by the presence of clustered metal–thiolate domains that we believe will have nanobiological properties. The α

domain was specifically chosen as it is generally more stable than the β domain. In this paper we initially explore the cadmium binding properties of chains of α domains, namely the α-, αα- and ααα peptides, but in future studies we will report on the properties of necklaces containing Cu–S and Ag–S clusters. Over the last 10 years we have demonstrated the utility of MM3/MD calculations in understanding the metal-induced folding in metallothioneins for the isolated domains and the native βα-MT protein. We extend those calculations using the proven force fields of Chan et al.[22] to model the flexibility expected for the necklaces with varying metal loadings. Figure 3 shows the energy minimised structures of the Cd_4α-rhMT, and the Cd_8αα-rhMT, and Cd_{12}ααα-rhMT concatenated proteins in typical "dumbbell" conformations. While the individual domains have been subjected to extensive MM3/MD relaxation calculations and the lowest energy structure was used, the concatenated structures shown here have not been subjected to extensive MM3/MD minimisation so they represent the 0 ps structures. The changes that take place following a series of MM3/MD calculations are shown in Figures 11–15 (see Results section). These first experiments aim to understand the overall metallation properties of these chains of domains by using electrospray mass spectrometry (ESI-MS), UV/Vis absorption and CD spectroscopy, with extensive molecular modelling to interpret these results. Our results also offer new insights into the application of chains of metal–thiolate clusters in biotechnological uses in the future, because, as is clear from the last figure in the paper, there is tremendous change in shape of these proteins as a function of the metallation status, change that can be harnessed in the future at the nanostructural level.

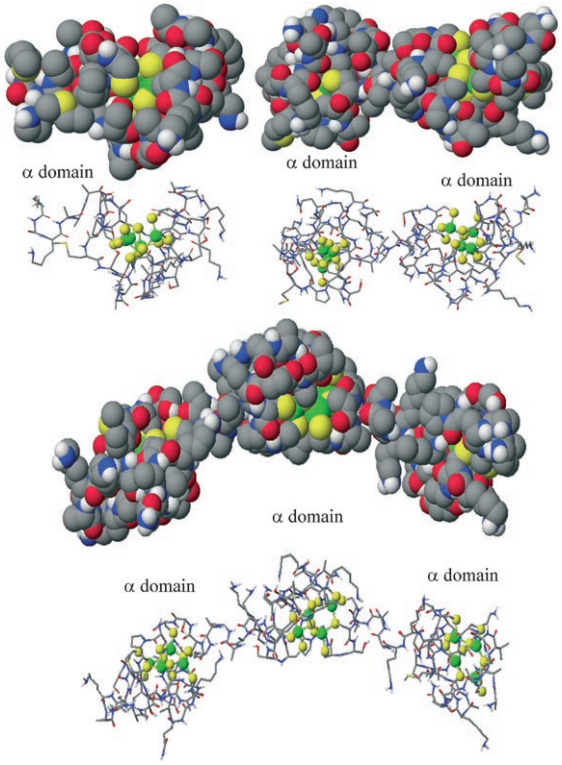

Figure 3. Three-dimensional, space-filling images of the cadmium-containing metallothionein structures studied by ESI-MS. These energy minimised structures of Cd_4-α-, Cd_8-αα-, and Cd_{12}-ααα-MT were calculated by using MM3 techniques[22] prior to the MD results shown in Figures 11–13, and should be compared with similar space-filling images, but after extensive MD calculations shown in Figures 14 and 15. The calculations may best be described as the ground state geometries at 0 ps. The ball-and-stick diagrams (below each space-filling image) show the alignment of the metal–thiolate clusters in each protein. The concatenated domains were formed by connecting N terminals to C terminals of the energy-minimised (MM3 and MM3/MD for 500 ps) individual domains. Atom legend: green = Cd^{II}, light yellow = S, gray = C, blue = N, red = O.

Results

Metal stoichiometry: The purified MT chains contained only Cd^{II} ions, hence, we could use the determination of SH group concentration by the previously reported methods[3] and the Cd^{II} ion concentration by atomic absorption spectrometry to determine the stoichiometries. A combination of these techniques gave the average Cd/S stoichiometry of the isolated proteins as 8.0 ± 0.1 for αα-rhMT1a and as 12.0 ± 0.1 for ααα-rhMT1a. ESI-MS spectra were recorded for each protein species at pH 7 and below pH 2.0 (Figures 4–6). Demetallation occurs near pH 3 (see below), so the comparison of the data for the species observed at pH 7 and pH < 2.5 provides the information required to calculate the total number of metals bound to each protein. The deconvoluted masses for Cd-containing α-rhMT1a, αα-rhMT1a and ααα-rhMT1a were in good agreement with the expected masses calculated according to their amino acid sequences and metallation by 4, 8 and 12 Cd atoms, respectively, as well as being coincident with the values obtained by the determination of SH group concentration and by atomic absorption spectrometry.

ESI-MS spectra of solutions of 11-cys α-rhMT1a, the 22-cys αα-rhMT1a and the 33-cys ααα-rhMT1a proteins at low pH and at neutral pH (Figure 4–6) show that there is a mixture of peptides present with the same number of SH groups and the same number of Cd^{II} ions, but with between 1–5 terminal residues missing, as indicated on the figures as "–A", "–2A", etc. This is most likely due to either post-source "nibbling" in the mass spectrometer or incorrect cleavage chemistry by the thrombin used to cleave the S-tag. We discuss this further in the Experimental Section. The missing residues play no part in the metal-binding properties of the protein. The CD spectra and UV absorption spectra for both the 22-cys αα-rhMT1a and the 33-cys ααα-rhMT1a (not shown) are typical of Cd_4-α domains[21] in exhibiting a derivative-shaped envelope centred on the thiolate-to-cadmium charge-transfer band at 250 nm.

ESI-MS data for the pH titration data for Cd_4-α-rhMT and Cd_8-αα-rhMT: Figure 7 shows the titration data for the single domain, Cd_4-α-rhMT between pH 1.8 and 7.0. The

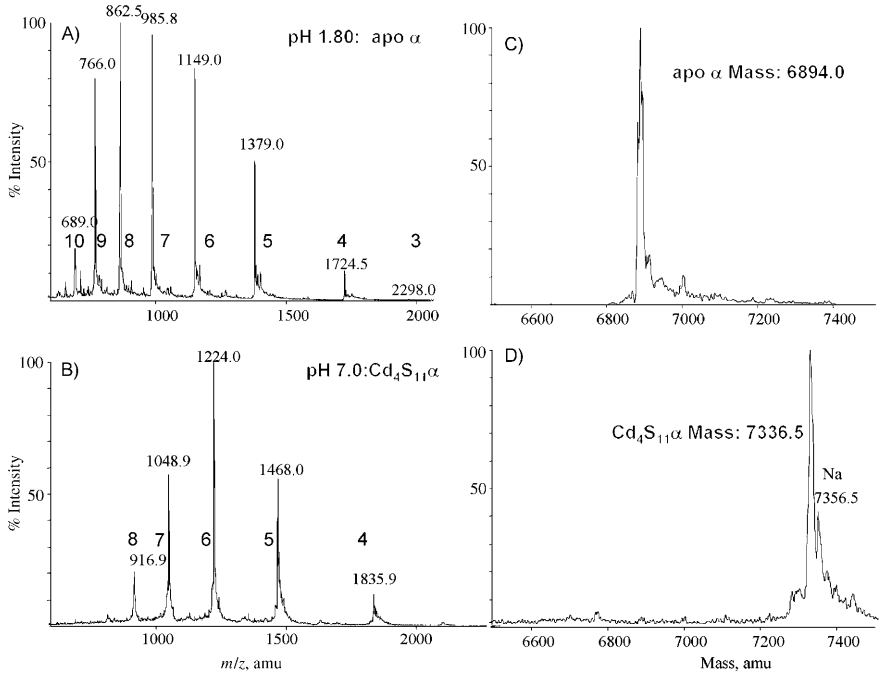

Figure 4. ESI mass charge-state spectra (A, B) and deconvoluted spectra (C,D) of recombinant human αMT1-a with S-tag at low (upper graphs) and neutral pH (lower graphs). In A) and B) the numerical ranges indicated show the charge state. In C) and D) the masses for the peptide containing zero and four Cd^{II} ions are shown, respectively.

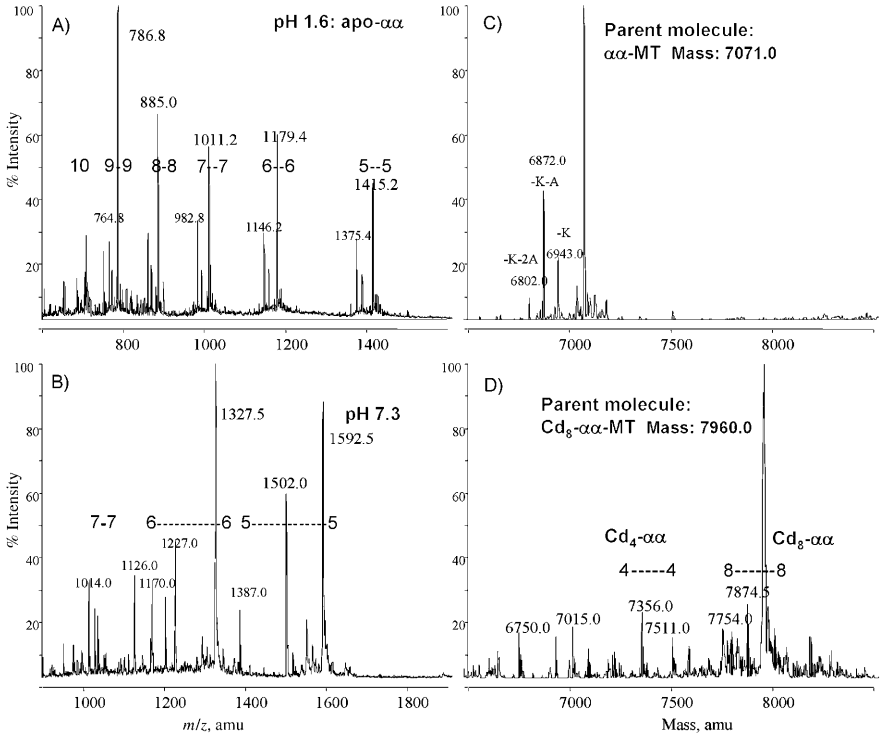

Figure 5. ESI mass spectra (A, B) and deconvoluted spectra (C,D) of recombinant human ααMT at low pH (upper graphs) and neutral pH (lower graphs). There is no S-tag attached to these peptides. In A) and B) the numerical ranges indicated show the charge state. In C) and D) the numerical ranges indicated show the masses for the peptide containing zero, four, eight, or ten Cd^{II} ions. In C) the sequence is shown for the parent ion, and the truncated species with 1–5 terminal residues lost most likely during during proteolytic cleavage ("nibbled").

data show that the protein only begins to demetallate in response to competition by the protons at pH 3.1 (Figure 7C, upper panel), in which the first indication of the major apo-α-rhMT charge states (+5 and +7) appear. The sequence shown in Figure 1A indicates possible basic sites for protonation for the charge states in blue. The deconvoluted spectrum (Figure 7C, lower panel) shows the mixture of apo-fully metallated. Complete demetallation has taken place by pH 2.6 (Figure 7B, lower panel), but the pH 2.60 charge-state data (Figure 7B, upper panel) show that an intermediate conformation exists with a charge-state maximum at +5 before the protein unwinds at pH 1.8 with a charge-state maximum of +7. The titration of the Cd_8-containing αα-rhMT with acid was followed by UV-visible absorption and circular dichroism spectroscopy and ESI-mass spectrometry. The Cd_8-αα-rhMT gives the known CD spectrum as in our previous studies[3,20,21] with no indication of intradomain interactions. The CD spectra diminish following addition of formic acid to the αα-rhMT1a solution as a result of demetallation (data not shown). The associated ESI-mass spectra (Figure 8) clearly show that demetallation takes place in a series of steps. Significantly, under the ESI-MS conditions used, and when measured with the pH decreasing from neutral to acidic, there is no indication of partially filled domains; however, the appearance of a Cd_4-αα species at pH 3.25, with continuing presence until pH 2.70, is evidence that the two domains are different in Cd-binding stability. In recent studies using very soft ESI-MS conditions and increasing the pH from acidic to neutral, we have measured partially

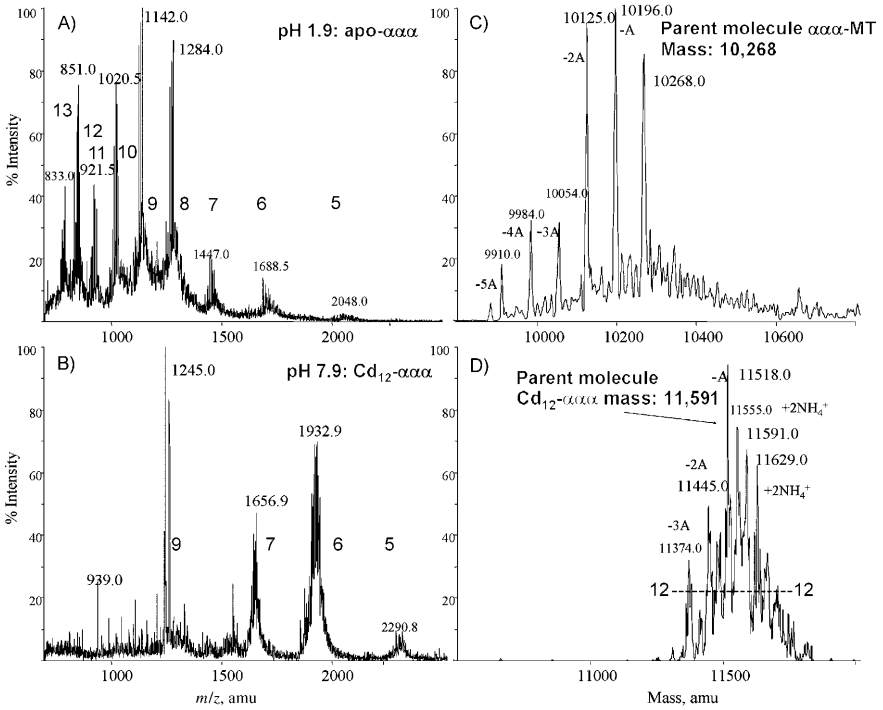

Figure 6. ESI-mass spectra (A, B) and deconvoluted spectra (C, D) of recombinant human αααMT at low pH (upper graphs) and basic pH (lower graphs). There is no S-tag attached to these peptides. In A) and B) the numerical ranges indicated show the charge states; for A) the range is +13 to +5, for B) +9 to +5 are identified. In C) and D) the numerical range indicated show the masses for the peptide containing 12 Cd^{II} ions. In C) the sequence is shown for the parent ion, and the truncated species with 1–5 terminal residues most likely lost during proteolytic cleavage ("nibbled"). The broadening in the charge states A) and B) is considered to arise from the increased salt and low protein concentrations used for the triple α-MT protein compared with the other peptides studied in this work.

metallated α-, β- and the complete βα-native rhMT1a protein species.[28,31] We show below by molecular dynamics (MD) that indeed the N-terminal and C-terminal α domains interact quite differently when demetallated. The charge states show that a conformation at pH 2.5 (+6 charge state dominant) is replaced by a low-pH conformation (at 1.6) with the +9 charge state dominant. The mass spectrum does indicate that there is a mixture, as the +6 charge state still accounts for significant fraction of the molecular species even at pH 1.6.

ESI-MS data for the pH titration of ααα-rhMT1a: The absorption and CD spectra of Cd_{12}-ααα-rhMT recorded as a function of pH show the same characteristics as for the single α domain, namely, the shoulder at 250 nm in the absorption spectrum, and the derivative, exciton-coupled CD spectrum centred on 250 nm (with a maxima at 260 and a minima at 240 nm) all diminish as the pH is lowered in response to proton-induced demetallation (data not shown).

The effect of pH on the metal-binding properties is more complicated when measured using ESI-MS. Figure 9 shows the charge-state ESI mass spectra recorded for Cd_{12}-ααα-rhMT between pH 7.9 and 1.90. The corresponding deconvoluted spectra are shown in Figure 10. Even from pH 7.9 to 3.50 (Figure 10E, F) the charge-state spectra show the presence of mixed conformations—the dominant charge states are +6, +7 and +9. The deconvoluted data show that only the fully metallated protein is present; the noise being contributed to by the effect of the neutral pH and the mixture of peptide lengths due to losses of residues (note that the mass scale for Figure 10A–C is shifted as a result of the loss of so many Cd atoms compared with the mass scale for the metallated species). At pH 3.33 (Figure 10D), the Cd_8 species appears with small amounts of the Cd_{12} species, but virtually no Cd_4 or metal-free protein. The +9 charge state is dominant. At pH 2.96 (Figure 10C) the protein has almost completely demetallated, only a very small fraction of Cd_4 remains. The charge states in Figure 9 panels A, B, and C show that the protein, even though demetallated, is very fluxional, with a number of conformations at the lowest pH (1.90) for which +12, +10, +9 and +8 are all dominant, replacing +9 and +6 at pH 2.56 and 3.0. The deconvoluted spectra at these pHs are the same, simply the demetallated, apo-ααα-rhMT. Significantly, there is no indication of the presence of partially metallated species, just the 4, 8, and 12 Cd-bound proteins. Clearly, also, the Cd_8 species is more stable with respect to competitive binding by protons than the first 4 Cd atoms. We address these experimental results with molecular dynamics results below.

Molecular models used to account for the spectroscopic data: We turn now to molecular dynamics to both understand the possible structural properties of these metallobiological necklaces and to begin the interpretation of the spectroscopic properties described above. We are particularly interested in predicting the most likely structure for all metallation states. These structures are extremely difficult to measure, but will provide insight into the proximity of the metal–thiolate domains with the concatenated structures and the location of the thiol units within the partially and fully demetallated peptides. The structures of the protein and its metal–thiolate clusters were obtained by using molecular mechanics and molecular dynamics simulation calculations. Models of α-rhMT1a, αα-rhMT1a and ααα-rhMT1a, as apo- and Cd_4, Cd_8 and Cd_{12} species, were constructed by

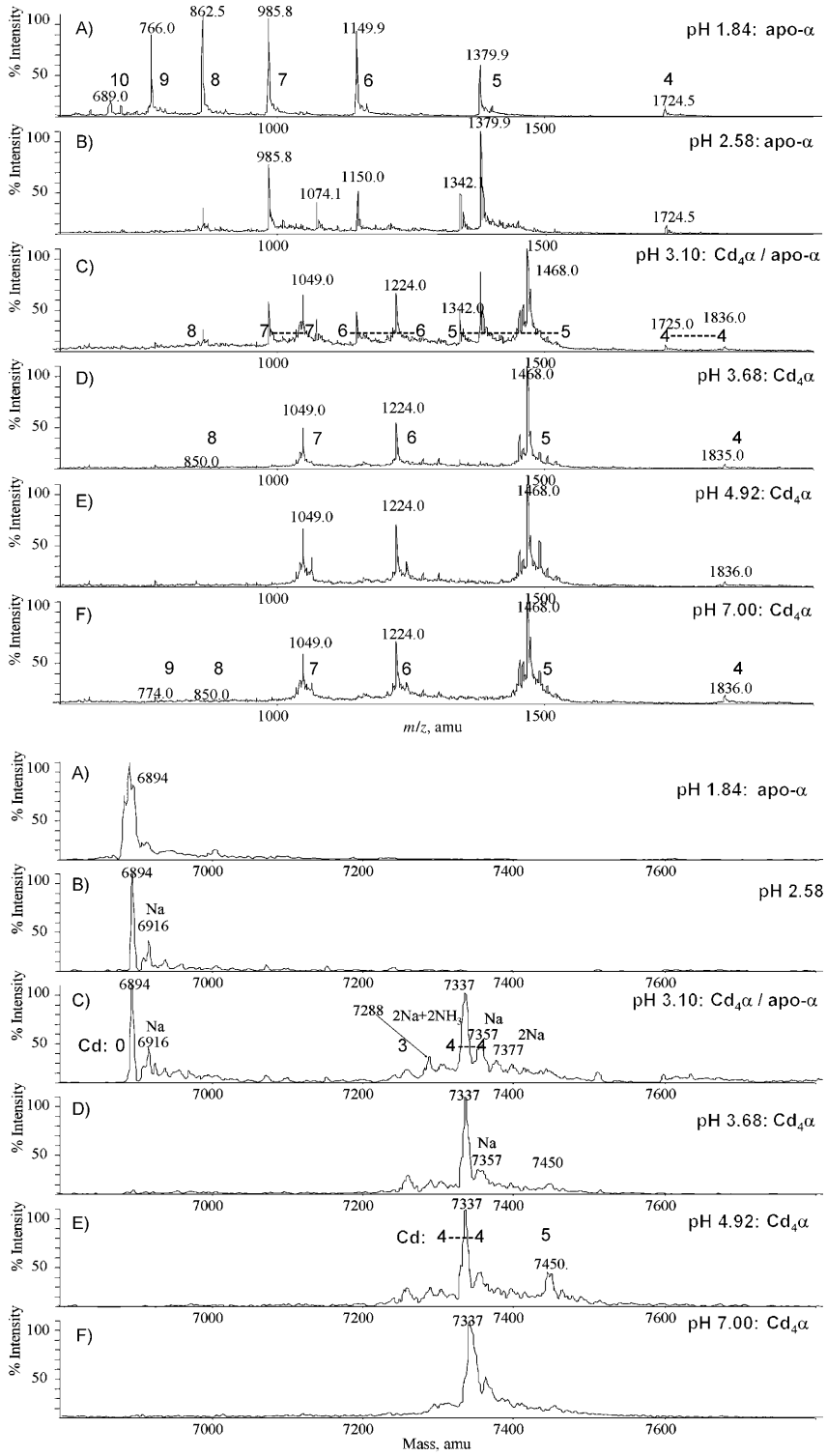

Figure 7. Effect of pH on the mass spectra of recombinant human αMT-1a. The upper panel of this figure shows the measured mass spectra (A–F) labelled with the charge states of the molecular species. The lower panel of this figure shows the reconstructed masses (A–F) that correspond to the measured mass spectra, as labelled. Metallation states of 0, 4 and 5 (trace) Cd^{II} are observed. Supermetallated Cd_5-α-MT has recently been reported by Duncan et al.[28] as a possible metal-transfer intermediate.

joining the Cd_4-α-MT structures head (N-terminus)-to-tail (C-terminus). The resulting strain was removed through a number of MM3/MD cycles over short (1–5 ps) time periods. Modified force-field parameters were defined for terminal or bridging sulfur atoms.[22] The molecular geometry was minimised by the molecular mechanics MM3 in CAChe 6.1.12 in the gas phase and followed by a cycle of molecular dynamics/molecular mechanics by using the conjugate gradient method and treating the methylene and methyl groups explicitly. Each of these calculations was carried out using the augmented MM3 force field provided by CAChe with specific modified parameters as described above.

Figure 3 shows the minimised structures for the fully metallated α-rhMT1a, αα-rhMT1a and ααα-rhMT1a proteins just after the first MM3 calculation had been completed, that is, prior to extensive MD calculations. The space-filling view provides an indication of the extent of encapsulation of the bound metals; the yellow spheres mark the cysteine metal-binding thiols. The ball-and-stick image provides a clear view of the cadmium–thiolate cluster structures. In these proteins there is a very short linker region between the domains. Chan et al.[22] have identified basic amino acid residues at which protonation can take place if the residue is exposed to the solvent. Protonation of some of these residues results in the charge states measured in the ESI-mass spectra shown in Figures 4–10. The ESI-MS data indicate the presence of multiple conformations, especially for the ααα-rhMT. To search for possible mixtures of conformations we carried out extensive molecular dynamics simulations on models of all the species identified in the ESI-mass spectra.

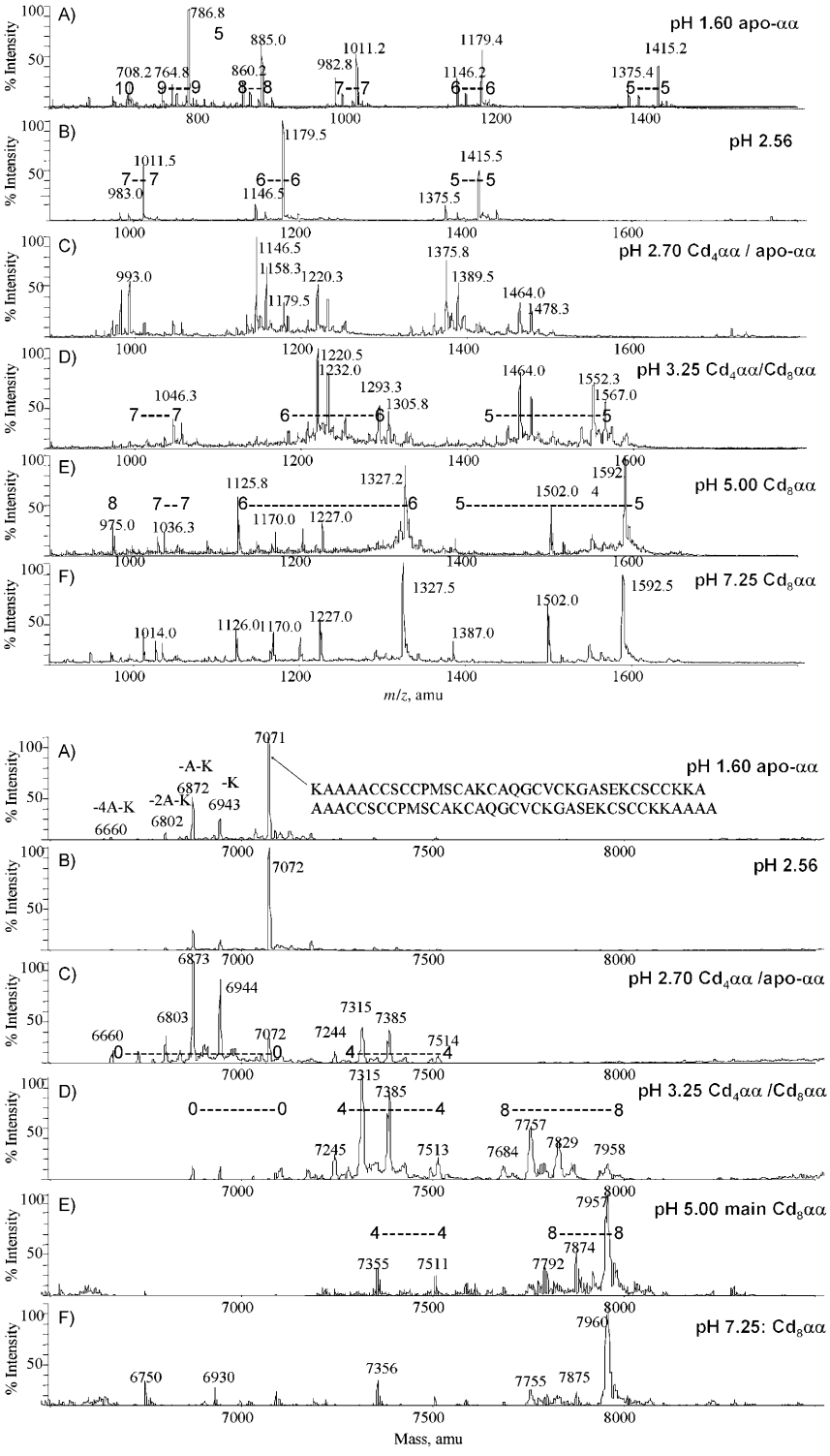

Figure 8. Effect of pH on the mass spectra of recombinant human ααMT-1a. The upper panel of this figure shows the measured mass spectra (A–F) labelled with the charge states of the molecular species. Note: The mass range in A) is shifted with respect to B)–F) because at low pH, higher charge states are observed (up to +10). The lower panel of this figure shows the reconstructed masses (A–F) that correspond to the measured mass spectra, as labelled. Metallation states of 0, 4 and 8 Cd^{II} are observed.

Molecular dynamics simulations of the demetallation reactions: Molecular dynamics simulations (MM3/MD) over 500 ps at 300 K were calculated for α-rhMT1a (details not shown, but reported previously as reference [23]), αα-rhMT1a (Figure 11), and ααα-rhMT1a, (Figures 12 and 13), starting from the structures shown in Figure 3 and using the same modified force-field as used in the MM3 energy minimisations. All atoms are considered in these simulations. The calculations were carried out twice and the overall results presented here were reproduced each time. The folding of the metal-free, apo-fragments has been reproduced in all peptides studied. The results described below provide insight into the flexibility of the protein at different metal-loading levels and the effects of the presence of up to three domains on these conformations. The most important results are that the two domain structures, usually shown as "dumb-bell" shaped, are, under MD conditions, seen as single, coalesced, globular conformations with intermingling of the domains to varying extents (see Figure 14). The completely demetallated proteins form completely globular structures with the thiols inverted from the core to face outward. On the other hand, when only the central domain, α_M, in the ααα species is demetallated, the two remaining domains separate as on a tether (Figure 15). We now describe these results in more detail.

MD calculations for αα-rhMT1a: Figure 11 shows the 3D structural conformers of αα-rhMT1a as a function of time at 300 K from MD energy/time trajectory snapshots. No MD results for such complicated metalloproteins have previously been reported and we are interested in understanding the relative influence of metallation in the N-terminal domain compared with the C-terminal domain. The natural human

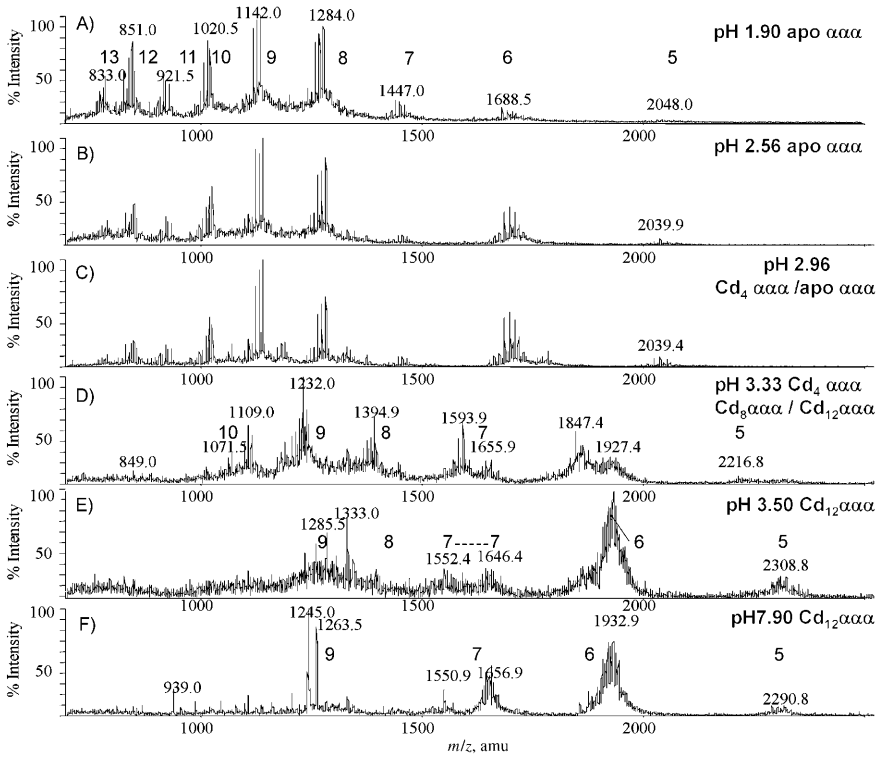

Figure 9. Mass-spectral charged-state data for recombinant human αααMT-1 recorded between pH 1.90 and 8.00. The primary parent molecules are indicated for each solution. pH of the solution is: A) 1.90, B) 2.56, C) 3.00, D) 3.33, E) 3.50 and F) 7.90. Note that the mass scale is different for A)–C) compared with D)–F), because the protein is much lighter at low pH. The corresponding deconvoluted spectra are shown in Figure 10.

metallothionein, βα-hMT has the β domain at the N-terminus and the α domain as the C-terminus. We show results for four specific species: 1) the fully metallated Cd_8-αα species, 2) the Cd_4-αα species, with demetallation of the N-terminal (Figure 11, left-hand side) domain, α_N; 3) the Cd_4-αα species, with demetallation of the C-terminal (Figure 11, right-hand side) domain, α_C; and 4) the Cd_0-αα species, with demetallation of both domains (apo-). Starting first with the fully metallated Cd_8-αα species: the two-isolated domains of the MM3-minimised structure moves over the 500 ps to coalesce into a single, loose globular structure with the linker extruded. Demetallating either domain singly also leads to a single structure, although demetallation of the α_C domain results in this occurring in the first 100 ps, whereas with demetallated α_N domain the peptides take much longer to associate. The fully demetallated protein also coalesces by 500 ps. These snapshots provide three major conclusions: First, the two domains interact completely, intertwining by 500 ps. Second, there is a difference in the extent of interaction depending on which domain is demetallated, in which the Cd_4-N-terminal domain in the very early stages of the MD simulation blends into the demetallated C-terminal domains. Third, the cysteinyl thiols all rearrange to move from the core of the domains to the surface of the domains, and the final structures are globular rather than linear as might be expected. In other words, there is, even if loose, structure for the metal-free domains. The final 500 ps- structures are compared in a space-filling view in Figure 14 in which the loss of the traditional "dumbbell" shape is evident. The intermingling of the two strands results in the much smaller volume occupied by the protein under all metallation states. Of significance is the coalescence of the metal-free, apo-αα-MT structure so that the 22 thiols are located on the outside of a compact globular structure.

MD calculations for ααα-rhMT1a: Figure 12 presents the 3D conformation of ααα-rhMT1a as a function of time at 300 K in MD energy/time trajectory snapshots. We show results for five specific species: 1) the fully metallated Cd_{12}-ααα species, 2) the Cd_8-ααα species, with demetallation of the N-terminal (Figure 12, left-hand side) domain, 3) the Cd_8-ααα species, with demetallation of the middle domain, 4) the Cd_8-ααα species, with demetallation of the C-terminal (Figure 12, right-hand side) and 5), in Figure 13, the Cd_0-ααα species, with demetallation of all three domains (apo-). Other combinations of domain-specific demetallation calculations were also calculated, but are not shown here. As for the αα domain, we find the general trend over 500 ps is for the domains to coalesce, losing their individual structures; however, the α_M and α_C domains interact far more than α_M and α_N domains, resulting in nonsymmetric associations. Quite different structures form for the Cd_8-α_C demetallated and the Cd_0-apo proteins.

Fully metallated—Cd_{12}-ααα-rhMT: The fully metallated Cd_{12}-ααα species moves over the 500 ps to coalesce into a loose globular structure with the linker extruded for the α_M and α_C domains, with α_N domain (Figure 12, left-hand side) clearly not associating. This association mimics that observed for the fully metallated αα protein (Figure 11), suggesting the hydrogen-bonding network is stronger for this interaction. Indeed, this behaviour is repeated when the α_N domain is demetallated: unusually for for the metal-free peptide, it does not closely associate with the remaining metallated peptide, rather it adopts a very loose structure.

Domain demetallation—Cd_8-ααα-rhMT: The minimised structures with one of each domain demetallated (α_N, α_M, α_C) show that there are significant differences depending on which domain is demetallated. We have calculated three var-

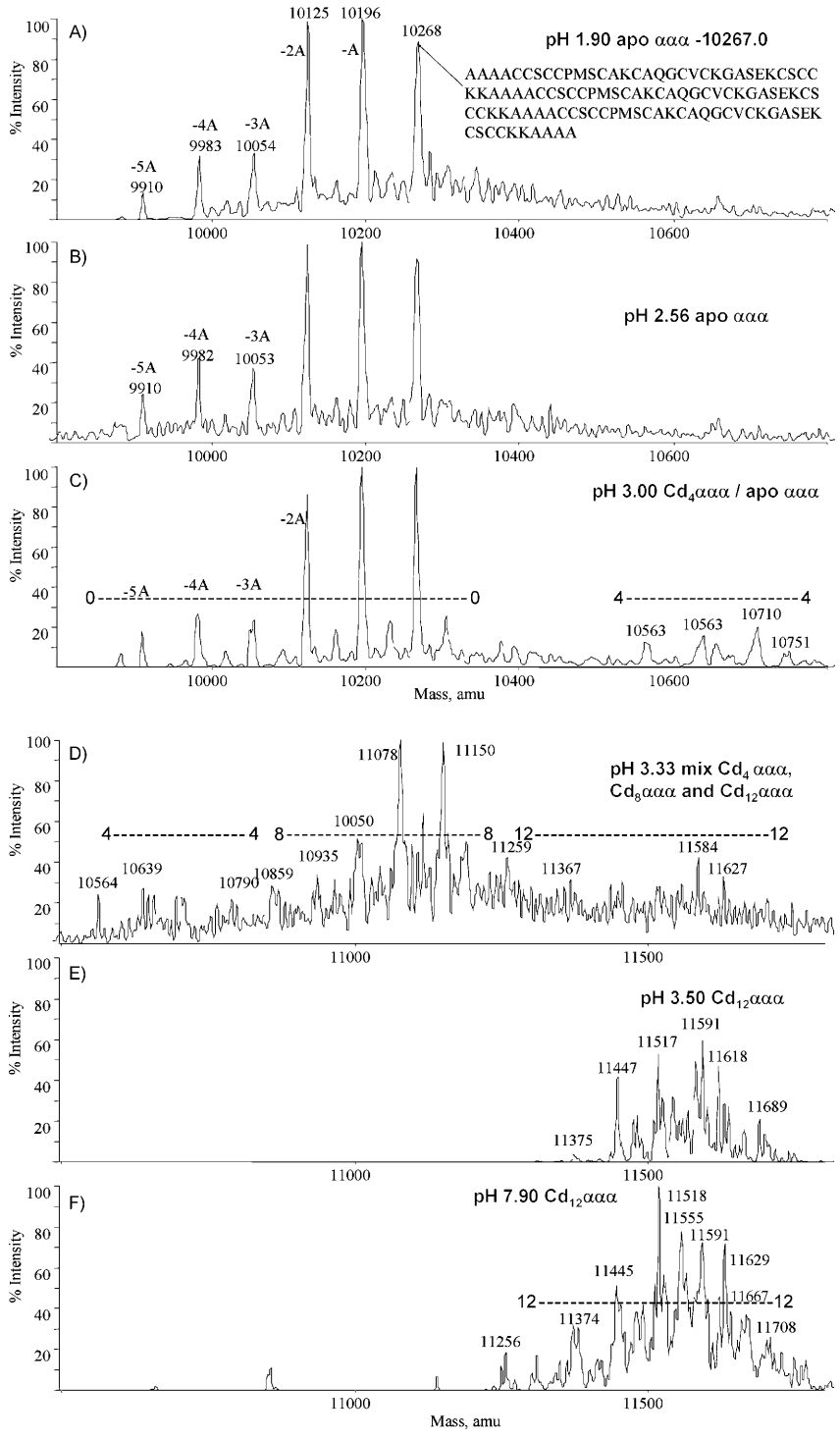

Figure 10. Reconstructed mass spectra for recombinant human αααMT-1a calculated species at pH 1.90–7.90. The different peaks are associated with loss of up to 5 alanine residues. Note that the mass axis is different for A)–C) compared with D)–F) because the Cd_{12} protein mass is centred on 11555 amu. Cd-loading of 0, 4, 8, and 12 is indicated on the spectra. The corresponding charge states are shown in Figure 9.

iants with Cd_8 loading: namely, by demetallating domain-D1 (α_N), the middle domain-D2 (α_M), and the third domain-D3 (α_C). The interaction behaviour of the protonated cysteines compared with the metallated cysteines is different for each of these. Considering first demetallation of the α_N domain, we find in Figure 12 that by 500 ps all three domains have interacted. In particular, the demetallated α_N domain coalesces with the middle domain (α_M), reducing the α_M–α_C domain interactions found for the fully metallated Cd_{12} protein. This domain specificity for domain–peptide interactions is clear in the structure that forms when α_C is demetallated (Figure 12). Now the α_N domain remains separate as in the case of the Cd_{12} protein and the α_M domain and metal-free α_C domain coalesce as in the fully metallated Cd_{12} protein. The inference from these two structures is that there is a head-to-tail effect on the metallothionein peptides that requires more study, but points to the differences in metal-binding properties between the β and α domains in the βα native proteins.

Demetallating α_M results in completely different behaviour. It can be seen from Figure 12 that at all times to 500 ps, the two metallated domains manoeuvre to stretch out the α_M section of the peptide, which results by the 500 ps point in an almost linear middle chain. However we should point out that even under these conditions there remains a folded loop at the α_N linking point; Figure 15 shows this clearly. This motion mimics that expected for two heavy domains connected by a long linker.

Domain demetallation—Cd_0-ααα-rhMT: Snapshots from the MD trajectory for the completely demetallated protein are shown in Figure 13. In the same manner as previously reported by Duncan & Stillman,[10] by 500 ps the protein completely coalesces and becomes intertwined.

These snapshots provide three major conclusions: First, the three domains interact completely differently. Second,

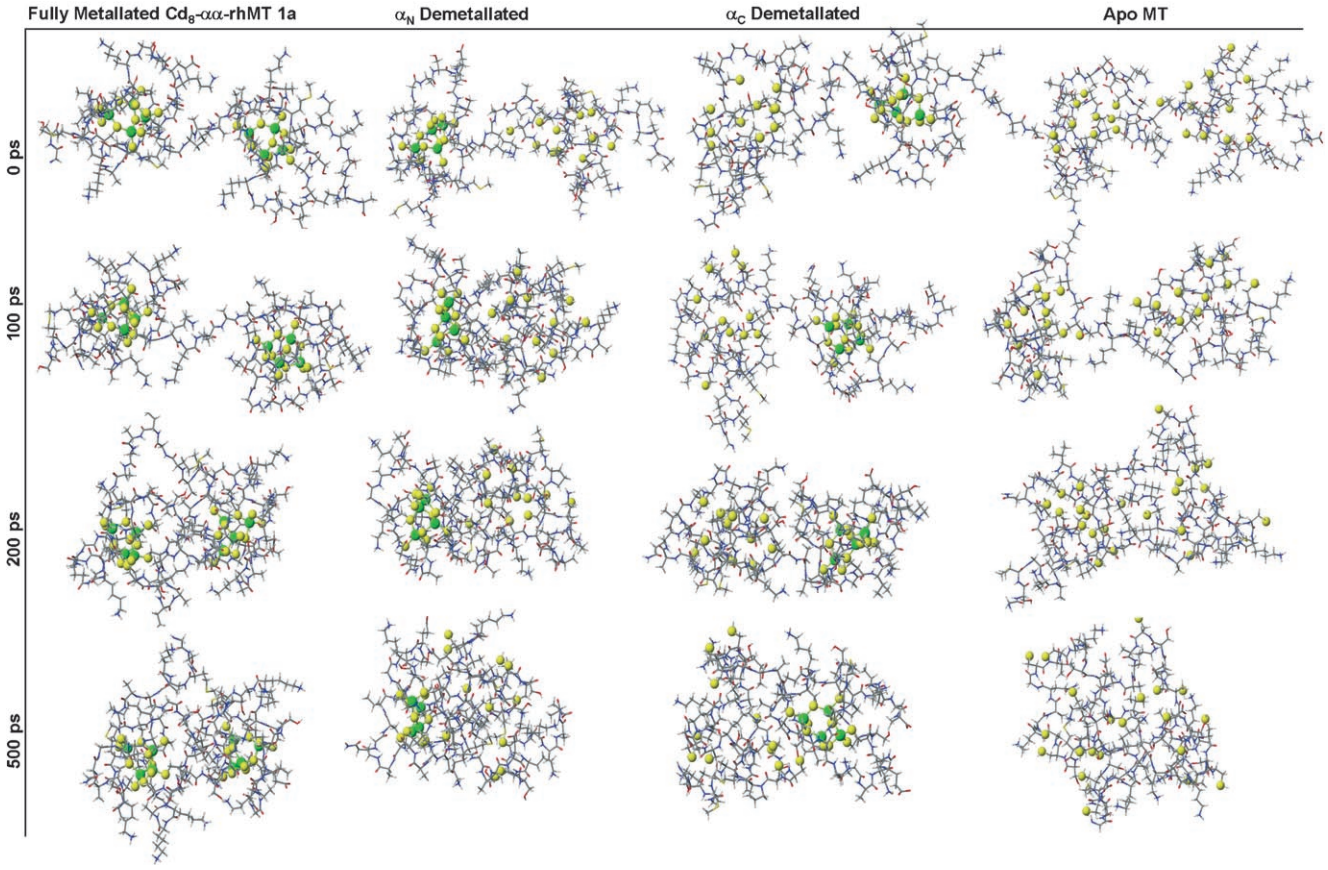

Figure 11. Conformers extracted from the MD trajectory of αα-rhMT1a showing the change in tertiary structure at 0, 100, 200, and 500 ps, simulated at a temperature of 300 K for Cd_8, Cd_0Cd_4-, Cd_4Cd_0- and Cd_0Cd_0-αα-rhMT1a. The protein strand is depicted as sticks and the cluster atoms are illustrated as balls. Atom legend: green = Cd^{II}, yellow = S, blue = N, red = O, black = C, grey = H. Space-filling images of the 500 ps-structures are shown in Figure 14. Note the loss of the two-domain, dumbbell structure of the 0 ps, energy-minimised ground-state structure shown in Figure 3.

there is a very significant difference in the extent of interaction depending on which domain is demetallated, particularly, demetallation of the α_M domain results in a completely open structure. Third, the cysteinyl thiol groups in the demetallated domains rearrange to move from the core of the domains to the surface of the domains, and the final structure of the apo-ααα protein is highly compact. In other words, there is some structure for the metal-free domains.

Finally, we show 3D-space-filling images in Figure 14. These images from the 500 ps point, more clearly emphasise the extent of folding and reorganisation of the cysteine thiol groups that accompanies demetallation. In Figure 15, we change the view of the middle domain so that its interaction can be seen more readily. What stands out is the very great change in overall dimension of the protein as a function of the metallation status.

Discussion

Metallothioneins have long been known for their remarkable metal binding properties, especially in the regulatory pathways of zinc and copper, and by default also cadmium.[1–15] A wide range of techniques has been used to characterise the metallation and demetallation properties for a number of metallothioneins from the different sources, in particular, ESI-MS, CD and NMR spectroscopy. Recently, ESI-MS has been employed in studies of a number of different metallothioneins.[16,23–27] Circular dichroism (CD) data have shown that the number of cadmium cluster species that form when Cd^{II} is added to metallothionein depends on the pH, temperature (between 0 and 60 °C), and the metallated state of the starting protein.[21] CD data, particularly, have indicated that the speciation of the metal depends on the molar ratio and the coordination geometry; Zn^{II} and Cd^{II} bind tetrahedrally[1–8] into well-formed metal–thiolate clusters almost completely wrapped by the peptide chain so that these clusters are well-shielded from the environment. These properties have led us to study the proteins described in this paper: proteins with chains of metal–thiolate clusters. Our objective is to understand the reasons for the presence of two domains in mammalian proteins, to understand differences in metal binding between the N-terminal domain compared with the C-terminal domains, to determine if chains of clusters can exist in a necklace fashion for use in biotechnology and to lead the way to the preparation of

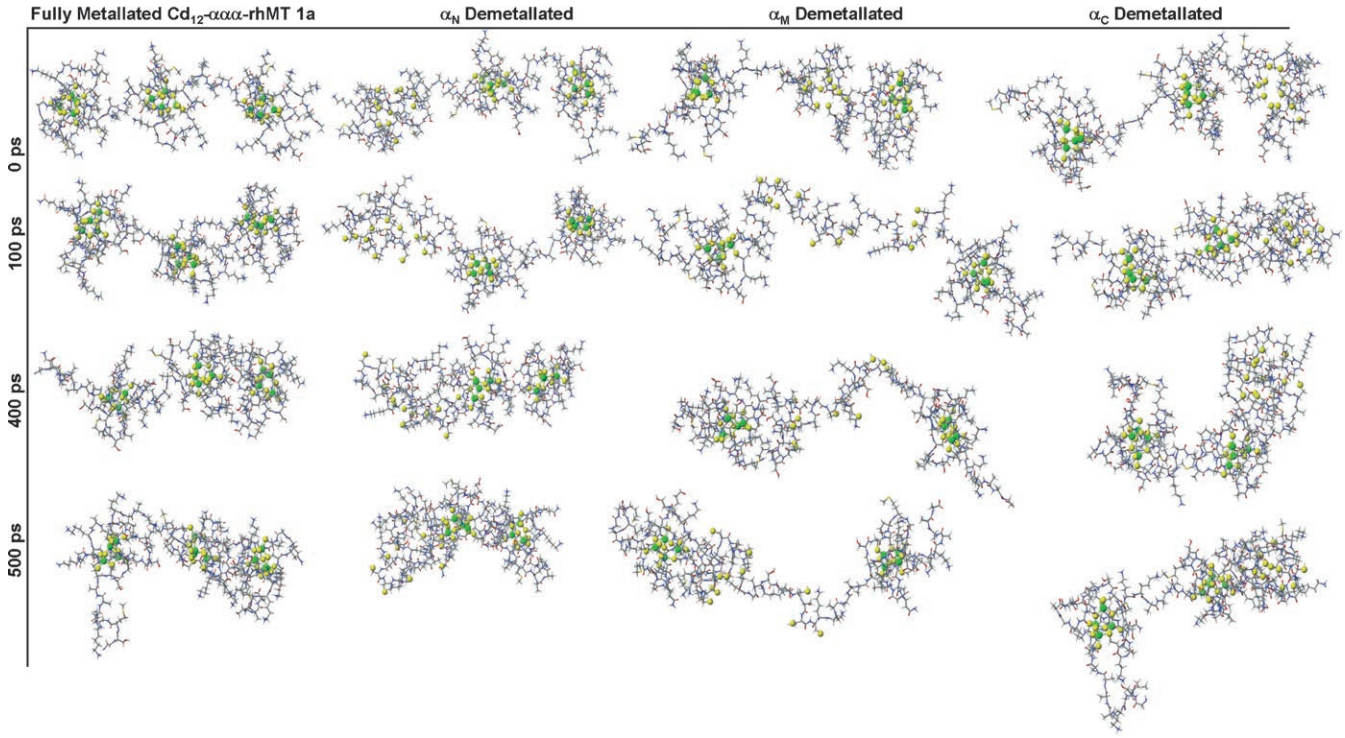

Figure 12. Conformers extracted from the MD trajectory change in secondary and tertiary structure of Cd_n-ααα-rhMT1a ($n=12$, 8, 8, and 8) at 0, 100, 400 and 500 ps with a simulated temperature of 300 K. Structures are shown for: Cd_{12}, $Cd_0Cd_4Cd_4$-, $Cd_4Cd_0Cd_4$- and $Cd_4Cd_4Cd_0$-ααα-rhMT1a. The results from the MM3/MD trajectory for the fully demetallated $Cd_0Cd_0Cd_0$-ααα-rhMT1a are shown in Figure 13. The protein residues depicted in ball-and-stick form and colour-coded by atom. The final structures are shown as space-filling images in Figure 14. Note: For the three domains, D1, D2, D3, we indicate which domain is demetallated by α_N for D1, by α_M for D2 and by α_C for D3. Atom legend: green = Cd^{II}, yellow = S, blue = N, red = O, black = C, grey = H.

strings of clusters with photoactive and electroactive metals, metals that commonly bind to metallothioneins.

To achieve these goals we needed to understand the metallation reactions of the domains when strung into chains. The best metal to study this with was cadmium, because it forms stable, tetrahedrally coordinated thiolate clusters with well-defined spectral properties. In addition, the force fields that describe bridging and terminal thiolate clusters have been tested and published.[22] Our study reports the combination of experimental data and molecular dynamics calculations that provide interpretation of the observed data. While modelling has been used in the past to describe the structure of the individual domains of metallothionein containing zinc, cadmium and copper,[1,21] this is the first time, as far as we know, that such extensive modelling investigation is reported in which the effects of domain metal occupancy on the overall protein structure has been studied and correlated with experimental data. Certainly, these are the first modelling results for chains of domains and they show detail not previously considered.

Observations from the ESI-MS data: The data from the ESI-MS study on the Cd binding in αα-rhMT and ααα-rhMT provides information that is complementary to information from CD and ^{113}Cd NMR spectroscopy. Mass spectrometry can be used to follow in situ reactions between MT and a metal in aqueous solution at any pH for the time period ranging from 2 min to several hours.[16] It is also possible to detect and differentiate partially metallated species (Cd_n-MT), that exist in solution simultaneously.[28] The ESI-MS experiment provides at its most basic, the mass of the protein and the metallation status, but we point out that the measurement is made under high vacuum so the MM/MD simulations replicate this environment. The sequence of amino acids in the domains of these proteins is known and confirmed by using the ESI-MS spectrum of the metal-free proteins at low pH. The low-pH mass spectra provide the exact mass of the protonated, metal-free peptide chain; for the parent αα peptide this is 7071.0 amu (Figure 5), while for the parent ααα peptide this is 10 268.0 amu (Figure 6). These values provide sufficient accuracy to allow the sequence to be determined if the theoretical sequence is known. The sequences calculated from the experimental data match those shown in Figure 1. For the cadmium-bound species, the parent αα fragment theoretical mass is 7954.0 amu and the experimental mass was determined as 7958.4 ± 0.7 amu. For the parent ααα fragment, the theoretical mass is 11 587.5 amu, while the experimental mass was determined as $11\,588.8 \pm 5.4$ amu. The two key types of data to be taken from the ESI-MS results are the changes in

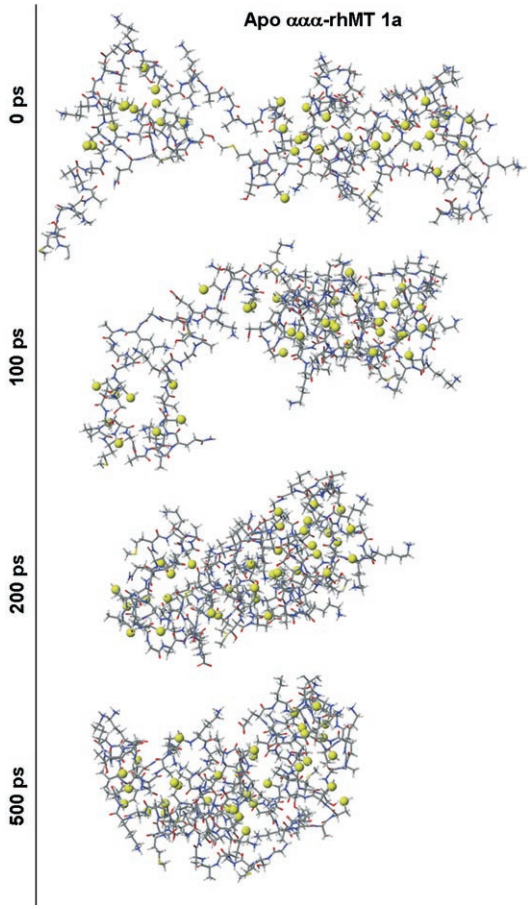

Figure 13. Conformers extracted from the MD trajectory change in secondary and tertiary structure of apo-$Cd_0Cd_0Cd_0$-ααα-rhMT1a at 0, 100, 200, and 500 ps with a simulated temperature of 300 K. The protein residues depicted in ball-and-stick form and colour-coded by atom. The final structures are shown as space-filling images in Figure 14. Atom legend: yellow = S, blue = N, red = O, black = C, grey = H.

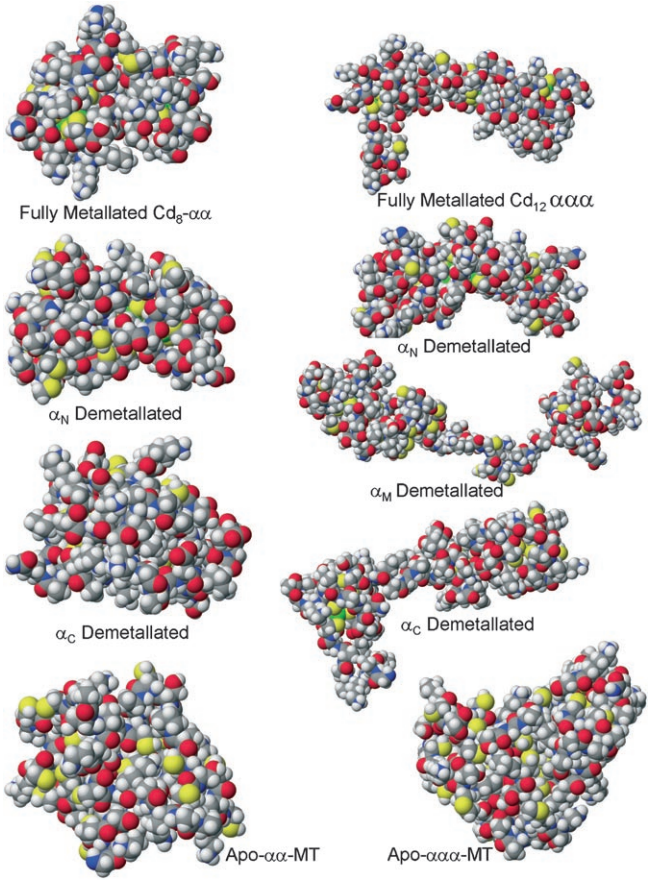

Figure 14. Space-filling views of the key Cd_n-αα-rhMT1a (left) and Cd_n-ααα-rhMT1a (right) protein species following MD for 500 ps.

charge state, which can be associated with the adoption of different conformations, and the relative stability of the clusters.

pH Titration of α-, αα- and ααα-rhMT1a: While the protein fragments used in this study were formed as the Cd-containing peptides, at pH 2.56, the Cd^{II} was completely displaced by the protons. CD data show that at low pH there is much less structure in the absence of metals (data not shown), as reported previously.[1,21] However the pH dependence of the mass spectra of the α, αα and ααα species (Figures 4–9) are noteworthy for the manner in which the charge states do not change as a function of Cd^{II} loading, but do change as a function of pH once the protein has been demetallated. The dominant charge state does not change by more than one unit between apo at pH just less than the demetallation point (about 2.6) and fully metallated states (from 5 upwards) for many of the ESI-MS spectra of metallothioneins, because, we suggest, the overall globular or spherical structure is maintained throughout the demetallation process. Chan et al.[23] have reported on the location of basic amino acid residues on the outside of the individual domain and the native βα-MT protein structures that are available for protonation (Figures 10 and 11 and Table 2 in reference [23]) allowing formation of the highly charged species observed by their charge states in the ESI-MS data. Calculations for the species described here provide very similar topographies, namely, located around the structures are a number of basic regions of the peptide chain.

Charge state data indicate presence of more unfolded conformation at low pH: In the experiments described here, we extended the pH towards 1.5 to examine possible denaturation effects amplified by the presence of two or three identical domains. As the data show, there are changes in the conformation for each protein below the demetallation pH and these changes are most significant in the ααα peptide. In all three peptides, at very low pH (Figures 4–6), the dominant charge state is +8 or +9, compared with the +6 at higher pH values. The new presence of the dominant charge state (+9 for αα and +12 for ααα species) at very low pH, suggests that there is another conformation that is more unfolded by the acidity (a well known denaturant). The ESI-MS data for the ααα peptide provides further evidence that this is property of the entire protein and requires complete demetallation. The +12 charge state at 851 amu replaces the

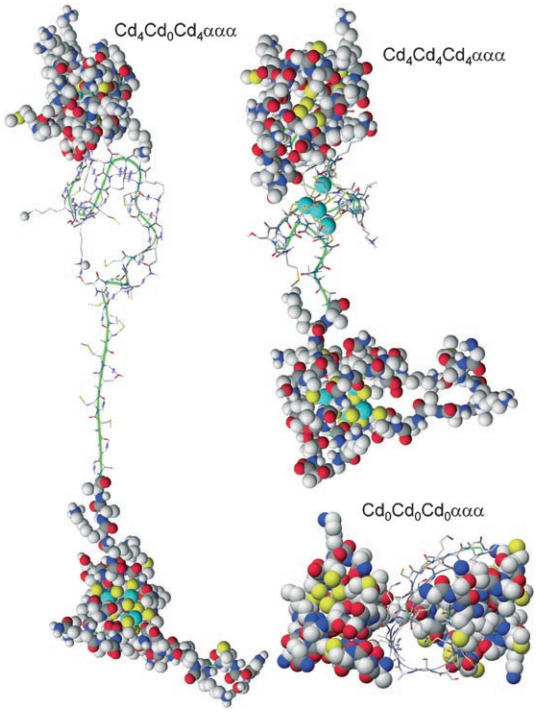

Figure 15. Space-filling views of the key Cd_n-ααα-rhMT1a protein species ($n=0$, 8, 12) following MD for 500 ps with the central domain drawn with just bonds and a ribbon to emphasise the spatial layout of the complete molecule. Note that the overall scale of the space-filling representations of the peptide chain and the ribbon representations are the same. For demetallation of the middle domain, the ribbon extends fully at 500 ps, whereas the middle domain peptide wraps close to the top domain for Cd_{12}- and intermingles with the right hand domain for Cd_0. Atom legend: turquoise = Cd^{II}, yellow = S, blue = N, red = O, black = C, grey = H.

+9 charge state at 1142 amu at pH 1.9. In separate experiments for the ααα peptide for which the S-tag was still attached (unlike here), we find that the +10 charge state at pH 7 for the Cd_{12} species is replaced by +16 for the metal-free apo species at pH 2.5, indicating that the underlying process is the unfolding of the domains at low pH.

Metallation status as a function of pH: We find from the detailed ESI-MS data described here unusual differences; first, the apparently identical domains demetallate at different acidities indicating the different stabilities and, second, conformations appear at low pH that are clearly more open than for similarly demetallated species but at higher pH values. From the pH titration of shown in Figures 7–10, proton competition results in demetallation over a very short range of pH. However, there is new detail in the pH titration studies. First, under these conditions, the αα protein loses one set of four Cd^{II} ions at a pH higher than the last set. The situation is more complicated with the Cd_{12}-ααα protein, because it appears that four Cd^{II} ions are lost at a much higher pH than the remaining eight Cd^{II} ions, indicating considerably reduced stability. Interestingly from a coordination chemistry viewpoint, demetallation takes place at solution acidities far below the pK_a of the cysteinyl thiolates. These experimental results may be understood by examining the computational results described that show both coalescence of the metal free domains and inversion of the orientation of the metal-binding cysteinyl thiols.

The energy minimisation of the structures of the clusters: The space-filling and tube representations of this minimised structure for Cd_4-α-, αα-, and ααα-rhMT1a are shown in Figures 11–14. While energy minimised α, β, and βα peptides have been previously reported,[23] there have been no reports of the structures of the concatenated domains. The calculations shown in Figures 11–14 provide interpretation of the ESI-MS results. The summary in Figure 15 illustrates the very significant change in structure predicted by the MM/MD calculations for the species studied by ESI-MS.

The MD results over 500 ps show an important feature of metallothioneins: there is a folding process that takes place for the metallated and metal-free peptides. Even for the fully metallated domains we find a coalescence of the domains. The linker between two domains in αα-rhMT1a moves so that each α domain approaches as a result of hydrogen-bonding and hydrophobic interactions.

There are two linkers that connect the three clusters in the ααα structure and we observe a rather different trend than in the αα structures. The linker between the middle (D2 or α_M) and C-terminal (D3 or α_C) clusters moves to allow α_M and α_C domains to intertwine, with the Cd_4-α_N domain left unaffected and exposed.

Demetallation: Molecular dynamics simulations were performed on the Cd-demetallated αα- and ααα-rhMT1a peptides. Figures 11–13 show that the conformers extracted from the MD trajectory change in secondary and tertiary structure in a dramatic but systematic manner. By 500 ps in each case for the αα peptide, we find that the domain residues are intertwined. However, while there is loss of the typical domain structure for the conformers of the ααα peptide following protonation of the three domains; all three domain residues do not interact until complete demetallation. Of significance, are recent reports that suggest a role for the metal-free apo-protein,[10–15] because the inversion of the thiol groups combined with the formation of the globular structure will provide stability for the thiol groups that might not be expected.

Figure 15 summarises the structures for the three different ααα-rhMT1a proteins described here. It is immediately apparent that our quest for a system that would exhibit metal-dependent structural change has been achieved. Each of the metallated species Cd = 0, 8, 12 exhibit dramatically different structures. In these remarkable views, the middle domain (α_M) has been drawn using just bonds and the ribbon superimposed. While the middle domain has been stretched, there still remains structure at the connection to α_N domain as is apparent from the ribbon. The second image is for the fully-metallated Cd_{12} ααα-rhMT protein, again, we have drawn the middle domain using just bonds and a ribbon, plus the four Cd^{II} ions. The close interaction

with the α_C domain (top in this view) is apparent. Finally, the bottom image, shows the overlap of the middle domain with both α_N and α_C domains. Here the demetallation allows the three domains to interact much more completely. The cysteinyl thiols are inverted from the core and face outward.

Conclusion

The ESI-MS data for a range of Cd-containing, 11-cysteine-α_n-MT peptides ($n=1$–3) show that metallation depends on the domain order in the chain. The pK_a of the coordinating cysteine residues is reduced to about 2.5. Demetallation of the just one domain in the ααα-rhMT protein can be seen as arising from loss of Cd^{II} from the middle domain, with the MM3/MD simulations indicating that the two remaining domains move apart. These results provide experimental and modelling support for the use of chains of metal–thiolate domains from metallothioneins for biotechnological applications in the future.

Experimental Section

Materials: The following chemicals were purchased: $CdSO_4$ (Fisher Scientific); kanamycin monosulfate (Sigma), LB agar (Sigma), LB broth (Sigma) and isopropyl-β-D-thiogalactopyranoside (IPTG) (Promega, UK); 5 mL Hi Trap™ SP Sepharose™ HP cation exchange cartridges (Pharmacia), and Sephadex G-25 Fine Grade (Pharmacia) were used for chromatography.

Protein preparation: The recombinant human metallothionein proteins used in this study were based on the α metal binding domain (α-rhMT1a, αα-rhMT1a and ααα-rhMT1a) with sequences shown in Figure 1A–C.[23] For αα-rhMT1a: KAAAACCSCCPMSCAKCAQGCVCKGASEKCSCCKKAAAACCSCCPMSCAKCAQGCVCKGASEKCSCCKKAAAA. For ααα-rhMT1a: AAAACCSCCPMSCAKCAQGCVCKGASEKCSCCKKAAAACCSCCPMSCAKCAQGCVCKGASEKCSCCKKAAAACCSCCPMSCAKCAQGCVCKGASEKCSCCKKAAAA. Parent molecule ααα protein mass: 10268. The recombinant proteins were engineered as S-tag™ (Novagen) fusion protein within a derivative of pET-29a placing the metallothionein directly downstream the thrombin cleavage site and over-expressed in BL21(DE3) strain of *E. coli* (Novagen). Plasmid constructs were transformed in a sterile environment. The transformed cells were cultured on fresh agar plates containing kanamycin and 50 μM $CdSO_4$ at 37 °C. LB broth containing kanamycin and 50 μM $CdSO_4$ was then inoculated with a colony from the agar plates. Expression was induced with the addition of IPTG. The $CdSO_4$ concentration was increased stepwise from 50 μM to 150 μM during the remaining four hours of incubation. The cells were harvested by centrifugation at 6000 rpm and then resuspended in 10 mM ammonium formate buffer containing mercaptoethanol to prevent oxidation. The cells were lysed by a French pressure cell and centrifuged at 13000 rpm to remove cellular debris. The supernatant was applied to the SP ion exchange cartridge, washed and then eluted with a NaCl salt gradient. The protein fractions from the SP cartridge were desalted on a superfine G-25 Sephadex column (100 cm), with elution by a 5 mM ammonium formate buffer. The fractions containing cadmium were subsequently identified by absorption spectroscopy (Varian Cary100), CD spectroscopy (Jasco J-810), AAS (Varian AA-875) and ESI-MS (PE-Sciex API 365). The purified protein fractions were collected, and then saturated with argon, sealed and stored in a freezer for use. All of the buffers used in the separation procedures were prepared using deionised water and argon saturated to prevent oxidation of the proteins. Samples used for analysis were slowly thawed and kept on ice and saturated with argon to prevent oxidation prior to analysis. The protein concentration in the thawed solutions was calculated from the cadmium concentration determined by AAS.

The S-tag in rfMT has the linkage sequence of LeuValProArg↓GlySer, which allows thrombin to cleave the S-tag. The fractions eluted off the SP cartridge were pooled, concentrated (stirred cell concentrator (Millipore) with regenerated cellulose YM3, 5000 molecular weight cut-off filter) and desalted (G-25 using 10 mM Tris-HCl buffer, pH 7.6), again pooled and concentrated. The cadmium concentration was analysed by atomic absorption spectroscopy (Varian AA-875). The thrombin was restriction grade purchased from Sigma. Thrombin (20 mg) was added to the protein (20 mg) and the solution was slowly stirred for 9 h at room temperature. This solution was then applied to an SP ion-exchange cartridge, washed with argon-saturated 10 mM Tris-HCl buffer made in deionised water to a pH of 7.40. The metallothionein was eluted with a solution of 95% 10 mM Tris-HCl buffer, pH 7.4, and 5% 10 mM Tris-HCl/1 M NaCl buffer, pH 7.4. These fractions were pooled, concentrated and desalted as above.

MT purification: Recombinant human α-rhMT1a, αα-rhMT1a, and ααα-rhMT1a prepared for these experiments have the sequences shown in Figure 1, with a linker region of four alanine residues to aid in the synthesis of the peptides.[23] The proteins were shown to be homogenous by the appearance of the single elution peak on the ion-exchange column and the expected amino acid composition from the ESI-MS data analysis. The metal-binding protein fractions were collected, desalted by gel permeation chromatography (Sephadex G25), and then characterised by the UV spectroscopy (data not shown; Varian Cary 100), the spectra of which display a broad band with a shoulder centred at about 250 nm typical of Cd–thiolate complexation, and by circular dichroism (Jasco J-810) in which the biphasic spectra are characteristic of clustered Cd_4–thiolate complexes in MT.

Protein and metal concentrations: The metal concentrations were determined with a Varian AA-875 series atomic absorption spectrophotometer. Protein concentrations were determined from measurements of SH groups by using Ellman's method, 5,5′-dithiobis-nitrobenzoic acid in 6.0 M guanidine hydrochloride[29] with a Cary-100 (Varian) UV/Vis spectrometer. Calculations were based on the assumption that eleven SH groups exist in the recombinant human α fragment.

ESI-MS parameters: The ESI-MS spectra were obtained using a PE-Sciex API 365 LC/MS/MS triple quadrupole mass spectrometer (PE-Sciex, Concord, Ontario, Canada). The protein samples were analysed in the positive ion mode by using the first quadrupole only. The analyte was infused into the atmospheric pressure interface (API) at 3 μL min^{-1}. Parameters for the spectra were as follows: an m/z range of 500 to 2300 amu, step size of 0.2 Da, dwell time of 0.3 ms, with ion source potential 5000 V, orifice potential 30 V, and ring potential 250 V. The solvent used in the analysis was a formate buffer, which was Ar saturated. All solutions were kept at 0 °C and Ar saturated. The mass calculations were performed using the program Biomultiview 1.5.1b, from the Biotools system (P.E. Sciex (Concord, Ontario, Canada)). We note that the "nibbled" peptides with masses missing a number of amino acid residues (for example, in Figure 6, we measure apo-ααα-MT with −1A to −4A, as alanine terminates the C-terminus we can identify the truncation to be at the C-terminus) most likely arise from a combination of the thrombin cleavage and processes occurring post-source in the mass spectrometer. We note that in a number of the figures, the peaks were very much broader than expected. We believe that the broadening arises from the use of the Tris buffer and low concentrations of protein near neutral pH. The Sciex ESI-MS instrument was not very sensitive under these conditions and the data were much poorer than measured at low pH. Similar problems occurred for the monomers; see, for example, reference [23].

pH Titrations of α-rhMT-1, αα-rhMT-1 and ααα-rhMT-1: The effect of pH on the folded structure of the Cd-containing binding proteins was evaluated through the changes observed in the UV absorption and CD spectra, and the ESI-mass spectrum following acidification with a 10 mM ammonium formate buffer, formic acid of HCl (for the most acidic solutions). The solutions were approximately 20 μM in 10 mM Tris buffer. The pH of each solution was measured directly with a digital pH meter. The conditions were the same as previously described.[23]

Computational methods: All calculations were performed using the CAChe Worksystem Pro 6.1.12 (Fujitsu America) using Allinger's MM3 force field[22,30] as augmented by CAChe and modified by us to included specific bond information for the Cd–S and Cd-S-Cd bonds formed in the clusters. Our procedures have been described previously.[10,11,22,23,28] The concatenation was carried out by bonding two or three Cd_4-α-MT domains in the correct head-to-tail alignment. The Cd-loaded domains were used to avoid tangling of the peptide chains. A series of MM3/MD cycles over 1–5 ps were carried out to relax the new coupling. Only when the structure minimised were the MM3/MD calculations carried out over the extended time periods. The calculations were repeated with different starting points resulting in the same overall structures. Results for the MM3/MD calculation of apo-α-MT have been published previously[28] and systematically folded into the globular shape reported here, Figure 13.

Acknowledgements

We acknowledge the financial support of NSERC of Canada (M.J.S.) and NATO for travel funds (to M.J.S. and PK), and CAChe, Fujitsu America, for providing the molecular modelling packages. We thank Prof. Lars Konermann (UWO) for use of the electrospray mass spectrometer, Prof. Mike Siu (York University, Canada) for discussion about the use of ESI-MS techniques with metallothioneins, and Dr Shengping Ma (MDS-Sciex, Canada) for assistance with the Biomultiview programs.

[1] M. J. Stillman, C. F. Shaw III, K. T. Suzuki in *Metallothioneins* (Eds.: M. J. Stillman, C. F. Shaw III, K. T. Suzuki), VCH, Weinheim, **1992**, pp. 1–12.
[2] J. H. R. Kagi, Y. Kojima, in *Metallothionein II, Chemistry and Biochemistry of Metallothionein* (Eds.: J. H. R. Kagi, Y. Kojima) Birkhauser, Basel, **1993**, pp. 25–63.
[3] M. J. Stillman, *Coord. Chem. Rev.* **1995**, *144*, 461–571.
[4] W. Braun, M. Vasak, A. H. Robbins, C. D. Stout, G. Wagner, J. H. R. Kagi, K. Wuthrich, *Proc. Natl. Acad. Sci. USA* **1992**, *89*, 10124–10128.
[5] A. H. Robbins, D. E. McRee, M. Williamson, S. A. Collett, N. H. Xuong, W. F. Furey, B. C. Wang, C. D Stout, *J. Mol. Biol.* **1991**, *221*, 1269–1293.
[6] A. H. Robbins, C. D. Stout, in *Metallothioneins* (Eds.: M. J. Stillman, C. F. Shaw III, K. T. Suzuki) VCH, Weinheim, **1992**, pp. 31–54.
[7] P. Schultze, E. Worgotter, W. Braun, G. Wagner, M. Vasak, J. H. R. Kagi, K. Wuthrich, *J. Mol. Biol.* **1988**, *203*, 251–268.
[8] J. D. Otvos, I. M. Armitage, *Proc. Natl. Acad. Sci. USA* **1980**, *77*, 7094–7098.
[9] M. J. Stillman, A. Presta, in *Molecular Biology and Toxicology of Metals*, (Ed.: R. K. Zalups, J. Koropatnick) Taylor and Francis, London, **2000**, pp. 1–33.
[10] K. E. R. Duncan, M. J. Stillman, *J. Inorg. Biochem.* **2006**, *100*, 2101–2107.
[11] K. E. R. Duncan, T. T. Ngu, J. Chan, M. T. Salgado, M. E. Merrifield, M. J. Stillman, *J. Exp. Biol.* **2006**, *231*, 1488–1499.
[12] I. Korichneva, *Antioxid. Redox Signaling* **2006**, *8*, 1707–1721.
[13] R. D. Palmiter, *Proc. Natl. Acad. Sci. USA* **1998**, *95*, 8428.
[14] A. Krężel, *W. Maret. J. Am. Chem. Soc.* **2007**, *129*, 10911–10921.
[15] C. Jacob, W. Maret, B. L. Vallee, *Proc. Natl. Acad. Sci. USA* **1999**, *96*, 1910.
[16] T. T. Ngu, M. J. Stillman, *J. Am. Chem. Soc.* **2006**, *128*, 12473–12483.
[17] T. Y. Li, A. J. Kraker, C. F. D. Shaw, D. H. Petering, *Proc. Natl. Acad. Sci. USA* **1980**, *77*, 6334–6338.
[18] J. H. R. Kagi, A. Schaffer, *Biochemistry* **1988**, *27*, 8509–8515.
[19] V. Calderone, B. Dolderer, H. Hartmann, H. Echner, C. Luchinat C. Bianco, S. Mangani, U. Weser, *Proc. Natl. Acad. Sci. USA* **2005**, *102*, 51–56.
[20] M. J. Stillman, W. Cai, A. J. Zelazowski, *J. Biol. Chem.* **1987**, *262*, 4538.
[21] M. J. Stillman, in *Metallothioneins. Synthesis, Structure and Properties of Metallothioneins, Phytochelatins and Metal–Thiolate Complexes* (Eds.: M. J. Stillman, C. F. Shaw, K. T. Suzuki), VCH, Weinheim, **1992**, Chapter 4, pp. 55–127.
[22] J. Chan, M. E. Merrifield, A. Soldatov, M. J. Stillman, *Inorg. Chem.* **2005**, *44*, 4923–4933.
[23] J. Chan, Z, Huang, I. Watt, P. Kille, M. J. Stillman, *Can. J. Chem.* **2007**, *85*, 898–912.
[24] J. A. Loo, R. R. Ogorzalek Loo, in *Electrospray Ionisation Mass Spectrometry* (Ed.: R. B. Cole), Wiley, New York, **1997** pp. 385–419.
[25] X. Yu, M. Wojciechowski, C. Fenselau, *Anal. Chem.* **1993**, *65*, 1355–1359.
[26] Y. J. C. Le Blanc, P. A. Presta, J. Veinot, D. Gibson, K. W. M. Siu, M. J. Stillman, *Protein Pept. Lett.* **1997**, *4*, 313.
[27] J. Chan, Z, Huang, M. E. Merrifield, M. T. Salgado, M. J. Stillman, *Coord. Chem. Rev.* **2002**, 233–234, 319–339.
[28] K. E. R. Duncan, M. J. Stillman, *FEBS J.* **2007**, *274*, 2253–2261.
[29] A. Presta, A. R. Green, A Zelazowski, M. J. Stillman, *Eur. J. Biochem.* **1995**, *227*, 226–240.
[30] N. L. Allinger, *J. Am. Chem. Soc.* **1977**, *99*, 8127.
[31] D. Sutherland, M. J. Stillman, *Biochem. Biophys. Res. Commun.* **2008**, *372*, 840–844.

Received: April 24, 2008
Revised: June 16, 2008
Published online: August 4, 2008

